EFFECTS OF ELECTRON AND PROTON DISTORTIONS IN THE (e, e'p) REACTIONS

BY V. V. GORCHAKOV*, V. K. LUKYANOV, YU. S. POL** AND B. L. REZNIK*

Laboratory of Theoretical Physics, Joint Institute for Nuclear Research, Dubna***

(Received May 19, 1973; Revised version received December 28, 1973)

The quasielastic (e, e'p) cross section has been derived taking into account the Coulomb distortion of electrons in the framework of the high energy approximation. In comparison with the plane wave approach, in the usual kinematics, the $d^4\sigma$ cross section of the ^{40}Ca (e, e'p) reaction increases in magnitude by 10–20% due to the electron distortion and decreases 3–4 times due to the inclusion of the proton optical potential. Then if one takes into account the diffuseness of nuclei in the hole-state dynamic-potential model, the $d^4\sigma$ cross section relatively increases 2–3 times in the energy range of 1p- and 1s-peaks.

1. Introduction

The mechanism of the quasielastic (e, e' p) process consists of scattering of an electron from a nuclear proton and transferring an amount of energy and momentum, so that the recoiled proton is thus emitted. The role of the other nucleons is reduced to the formation of the Coulomb and nuclear potentials, which distort the electron and proton wave functions. Such a reaction is a good tool in studying the momentum distributions, widths, and energies of the hole nuclear states [1]. Thus, the Amaldi group experiments [2] showed that the protons were knocked out from the 1d, 2s, 1p, and the lowest 1s nuclear shells. The energy of the latter happened to be of the order or lower than the depth of the usual potential well used in one-particle calculations.

In principle, the $d^4\sigma$ cross sections measured in the double coincidence experiments, detecting both the outgoing proton and the electron angles and energies [2], are of great interest. However, usually only the simple $d^2\sigma$ and $d^3\sigma$ cross sections are analyzed theoretically for all the light nuclei not heavier than ^{40}Ca. First, this is due to the existence of many experimental data on only these cross sections. Then, for the light nuclei it is possible to use the simple one-particle wave functions, choosing them by fitting the form and spin-

* On leave from Far East State University, Vladivostok.

** On leave from The Lebedev Physical Institute AN USSR, Moscow.

*** Address: Laboratory of Theoretical Physics, Joint Institute for Nuclear Research, Head Post Office, P. O. Box 79, Moscow, USSR.

-orbital part of the nuclear potential [3]. The more significant consideration [4] is based on the shell model calculations, including those for the residual particle-hole interactions. In this case the widths of the hole states are non-vanishing, therefore the $d^4\sigma$ cross section can be calculated [5].

In deriving the $(e, e'p)$ cross section one usually uses the first Born approximation with plane waves for the electrons and distorted waves for the knocked-out protons. However, it is obvious that in the case of medium and heavy nuclei the Coulomb distortion of the electron wave functions should have an effect.

The purpose of this work is to investigate the distortion effects in both the proton and the electron channels. To take into account the electron distortions, the so-called high energy approximation has been applied, and the $d^4\sigma$ cross sections have been calculated for the $(e, e'p)$ reaction on ^{40}Ca [2], the heaviest nucleus investigated experimentally. In the framework of the method suggested, the structure part of the whole matrix element may be considered independently in terms of any appropriate nuclear model. At the moment we use the resonance energies E_ν and widths Γ_ν, which were given in Refs [6, 8] and were found to be rather close to those observed experimentally [2]. The calculations of these values were carried out with the help of the so-called dynamic potential model [7], and the $(e, e'p)$ reaction itself was considered in the plane wave approximation for all particles e, e' and p [8]. In the framework of this model an account of nucleon-nucleon correlations leads to the non-local potential well, which in the first order of $(E-E_F)$ depends linearly on the state energy $E = E_\nu$ which is of interest (E_F is the Fermi energy). The resonance widths have been expressed through an imaginary part of the corresponding optical potential, and have also been calculated in Ref. [8].

2. *Derivation of the cross sections*

If we consider the nucleus A as an external field, the cross section of the reaction $(e, e'p)$ with the final state, consisting of an electron of momentum $\vec{k}_{e'}$ and a proton of momentum $\vec{p}$, is written in the form:

$$d^4\sigma = \frac{E_e}{k_e} \overline{\sum_{(if)}} |\tau_{if}|^2 \frac{d\vec{p}d\vec{k}_{e'}}{(2\pi)^6}, \tag{1}$$

where $\overline{\sum_{(if)}}$ is the average over the initial states and sum over the final states; and k_e/E_e is the incident flux of electrons ($\hbar = c = 1$) which in usual experiments ($E_e \gg m_e c^2$) is equal to 1. The reaction matrix element τ_{if} is expressed through the amplitude T_{if} on the energy shell:

$$\tau_{if} = -2\pi\delta(E_e - E_{e'} - E_p - \varepsilon)T_{if}. \tag{2}$$

Here we take into account the fact that the transferred electron energy $\omega = E_e - E_{e'}$ is distributed between the proton kinetic energy E_p and the residual nucleus $(A-1)$ energy:

$$\varepsilon = E^r + E^b + E = E_e - E_{e'} - E_p. \tag{3}$$

This latter is measured in the experiments by detecting the incident and outgoing particle energies E_e, $E_{e'}$ and E_p. Then, E^b is the proton bound energy; E is the nucleus $(A-1)$ excitation energy; and $E^r = q^2/2m_{A-1}$ ($\vec{q} = \vec{k}_e - \vec{k}_{e'}$) is its recoil energy, which can be neglected.

The observed $d^4\sigma$ cross sections [2] have wide resonances around the energies $\varepsilon = \varepsilon_v$, corresponding to the hole nuclear states with $E \sim E_v$. The latter are displayed at high nuclear energies (dozen MeV) and their amplitudes have a typical pole dependence in the region around $E = E_v + i\Gamma_v/2$. Then, using the usual average of Eq. (2) over an experimental resolution $\Delta E \ll |E_v - E_{v'}|; E_e; E_{e'}$, then reaction matrix element becomes of the following resonance form:

$$\tau_{if} = -2\pi \left(\frac{\Gamma_v}{2\pi}\right)^{1/2} \frac{1}{E - E_v - i\Gamma_v/2} T_{if}, \tag{4}$$

so that the cross section (1) is transformed into:

$$d^4\sigma = \frac{2\pi\Gamma_v}{(E-E_v)^2 + \Gamma_v^2/4} \overline{\sum_{(if)}} |T_{if}|^2 \frac{d\vec{p}\, d\vec{k}_{e'}}{(2\pi)^6}. \tag{5}$$

Keeping only the Coulomb term of the electromagnetic interaction potentials, the reaction amplitude is given by

$$T_{if} = e^2 \int d\vec{r} d\vec{x} \langle \Phi_{A-1}; \vec{p} | \hat{\varrho}(\vec{x}) | \Phi_A \rangle \Psi_f^+ \Psi_i \frac{e^{i\omega|\vec{r}-\vec{x}|}}{|\vec{r}-\vec{x}|}, \tag{6}$$

where $\Psi_{i,f}$ are the electron wave functions and ϱ is the nuclear charge density. The nuclear matrix element depends on the nuclear wave function of the initial Φ_A and of the final Φ_{A-1} states, and also depends on the outgoing proton wave function in the optical potential of the nucleus $(A-1)$.

As was shown in Refs [9, 10], the Coulomb distortion of the electron wave functions can be taken into account in the framework of the high-energy approximation ($E \gg U$, $kR \gg 1$), which is justified in the usual experiments with electrons [9–12]. It follows from Refs [9, 10] that

$$\Psi_f^+ \Psi_i = g(\vec{r}) e^{i\vec{q}\vec{r} + i\Phi(\vec{r})}. \tag{7}$$

The correction amplitude g, which depends also on the initial and final state spinors, and phase Φ are given in the Appendix. Replacing $\vec{u} = \vec{r} - \vec{x}$ in Eq. (7) and using an expansion on $|\vec{u}|/|\vec{x}| \ll 1$ of the functions [11]

$$\begin{aligned} g(\vec{x}, \vec{u}) &= g(\vec{x}) + \ldots, \\ \Phi(\vec{x}, \vec{u}) &= \Phi(\vec{x}) + \vec{\nabla}\Phi(\vec{x}) \cdot \vec{u} + \ldots, \end{aligned} \tag{8}$$

it is possible to integrate over $\vec{u}$. Thus

$$T_{if} = 4\pi e^2 \int d\vec{x} \frac{g(\vec{x})}{q_{\text{eff}}^2(\vec{x}) - \omega^2} \langle \Phi_{A-1}; \vec{p} | \varrho(\vec{x}) | \Phi_A \rangle e^{i\vec{q}\vec{x} + i\Phi(\vec{x})}, \tag{9}$$

where

$$\vec{q}_{\text{ef}} = \vec{q} + \vec{\nabla}\Phi(\vec{x}), \quad \vec{q} = \vec{k}_e - \vec{k}_{e'}. \tag{10}$$

Furthermore, we represent the nuclear matrix element as follows

$$\langle \Phi_{A-1}; \vec{p} | \varrho(\vec{x}) | \Phi_A \rangle = \sum_{lm} \varrho^{\nu}_{lm}(x, \vec{p}) Y^*_{lm}(\hat{x}), \tag{11}$$

where ϱ^{ν}_{lm} is expressed through the hole state wave function

$$\varphi_{\nu}(\vec{x}) = \langle \Phi_{A-1} | \Phi_A \rangle = R_{NL}(x) Y_{LM}(\hat{x}). \tag{12}$$

Here $\nu = NLM$ indicates the resonance index. The wave function of the knocked-out proton has the form:

$$|\vec{p}\rangle = 4\pi \sum_{\lambda M'} i^{\lambda} \chi_{\lambda}(px) Y_{\lambda M'}(\hat{x}) Y^*_{\lambda M'}(\hat{p}), \tag{13}$$

where χ_{λ} is the solution of the radial equation with the optical potential. (In the plane wave approximation $\chi_{\lambda} = j_{\lambda}(px)$.) Then, using the nuclear charge density with the point proton charges $\varrho(\vec{x}) = \sum \delta(\vec{x} - \vec{x}_i)$, we obtain:

$$\varrho^{\nu}_{lm}(x, \vec{p}) = \sqrt{4\pi(2l+1)(2L+1)}\, R_{NL}(x) \times$$

$$\times \sum_{\lambda M'} \frac{1}{i^{\lambda}\sqrt{2\lambda+1}} \chi_{\lambda}(px) Y^*_{\lambda M'}(\hat{p}) (lL00|\lambda 0) (lLmM|\lambda M'). \tag{14}$$

It was shown in Ref. [12] that the main contribution to a typical integral such as (9) comes from the expansion terms with projection $m = 0$ in Eq. (11) (neglecting the terms $O(1/kR)$). Then, we define:

$$\varrho^{\nu}(\vec{x}, \vec{p}) = \sum_{l} \varrho^{\nu}_{l0}(x, \vec{p}) \sqrt{\frac{2l+1}{4\pi}} P_l(\mu),$$

$$\mu = \cos(\hat{x}, 0z) \tag{15}$$

and the amplitude (9) becomes:

$$T_{if} = 4\pi e^2 \int_0^{\infty} x^2 dx \int_0^{2\pi} d\varphi \int_{-1}^{1} d\mu \left\{ \frac{g(\vec{x})}{q^2_{\text{ef}}(\vec{x}) - \omega^2} \varrho^{\nu}(x, \mu, \vec{p}) e^{i\Phi(\vec{x})} \right\} e^{i\vec{q}\vec{x}}. \tag{16}$$

In order to carry out the following calculations we choose a coordinate system with an axis $0z$ along $\vec{q}_1$, where

$$\vec{q}_1 = \vec{k}_1 - \vec{k}_2, \quad k_1 = k_2 = k = (k_e + k_{e'})/2,$$

$$\vec{k}_1 = \vec{k}_e - \hat{k}_e \bar{q}, \quad \vec{k}_2 = \vec{k}_{e'} + \hat{k}_{e'} \bar{q}, \quad \bar{q} = (k_e - k_{e'})/2 = \omega/2. \tag{17}$$

Then

$$\cos(\widehat{k_e x}) = \alpha\mu + \sqrt{1-\alpha^2}\cdot\sqrt{1-\mu^2}\cdot\cos\varphi,$$

$$\cos(\widehat{k_{e'} x}) = -\alpha\mu + \sqrt{1-\alpha^2}\,\sqrt{1-\mu^2}\cos\varphi \tag{18}$$

where $\alpha = \sin\vartheta/2$ and where ϑ is the electron scattering angle. Now the integral over μ in Eq. (16) can be written as follows:

$$\mathcal{I}(x, \varphi) = \int_{-1}^{1} d\mu F(x, \mu, \varphi) e^{ikxf(\mu,\varphi)}, \tag{19}$$

where

$$f(\mu, \varphi) = 2\alpha\mu + 2\frac{\bar{q}}{k}\sqrt{1-\mu^2}\,\sqrt{1-\alpha^2}\cos\varphi. \tag{20}$$

Note that in the region of main contribution $kx \sim kR \gg 1$ of Eq. (19), the function $F(x\mu\varphi)$ depends smoothly on μ in comparison with the quickly oscillated exponential function. Therefore one can integrate in Eq. (19) with the help of the stationary phase method. The stationary point is calculated from equation $f'(\mu_0) = 0$, which gives

$$\mu_0 = \left(1 + \frac{\bar{q}^2(1-\alpha^2)}{k^2\alpha^2}\cos^2\varphi\right)^{-1/2}. \tag{21}$$

It is a significant result that at this point, as can be seen in the Appendix, the functions g, φ and q_{ef} do not depend on φ at all. This permits the next integration over φ to be performed. Thus the final result for the reaction amplitude is

$$T_{if} = -\frac{2\pi^2 e^2 \Phi(i\sqrt{2\pi})}{\sqrt{k}\cdot\bar{q}\cdot\sqrt{\alpha(1-\alpha^2)}}\int_0^\infty dx\sqrt{x}\,\frac{g(x\mu_0)}{q_{\text{ef}}^2(x\mu_0)-\omega^2}\,\varrho^{\nu}(x, \mu_0, \vec{p})\times$$

$$\times\exp i\left[2kx\alpha + \frac{\bar{q}^2(1-\alpha^2)}{k\alpha}x + \Phi(x\mu_0)\right], \tag{22}$$

where $\Phi(i\sqrt{2\pi})$ is the Frenel integral. The functions g, Φ and q_{ef} are well-known (see Appendix), and ϱ^{ν} is formed with the help of the hole state and the outgoing proton wave functions. Future calculations of Eq. (22) can therefore be easily performed numerically.

3. Results and discussion

The cross section $d^4\sigma$ of the quasielastic electron scattering on ^{40}Ca were calculated with the help of Eqs (5) and (22) at kinematic conditions corresponding to the first experiment where angles and energies of outgoing particles were fixed as [2]:

$$E_{e'} = 470\text{ MeV}, \quad E_{\text{p}} = 116\text{ MeV}, \quad \vartheta_{e'} = 51°, \quad \vartheta_{\text{p}} = 62° \tag{23}$$

(the spectra of electron-proton coincidences). In this experiment the incoming electron energy was varied and the cross sections were measured as a function of energy ε transferred to the nucleus and defined by Eq. (3).

The resonance positions corresponding to the excitation energies of the hole states were determined in this reaction with a rather large error and the peaks are actually difficult to identify. Nevertheless, by summing up the results of a number of papers [13–15] and the conclusions given by their authors, it is possible to assign the following energy bars to these peaks:

$$E_{1s} = 45 \div 60 \text{ MeV}, \quad E_{1p} = 28 \div 43 \text{ MeV}, \quad E_{1d} = 13 \div 18 \text{ MeV}. \tag{24}$$

One can see that at least the 1s-proton separation energy E_{1s} turns out to be larger than the potential well depth commonly used in the shell-model calculations. This fact is usually interpreted as the hollow effect of a hole potential.

In the present paper the energies and the widths of those states have been calculated in the framework of the model of Ref. [6, 7], which makes use of the field theoretical methods in the many-body nuclear problem. In the model the hole potential parameters prove to be energy dependent. As was shown in Ref. [8], this energy dependence can be given with a good accuracy as follows

$$U(x) \doteq -V \cdot \theta(x-R)\{1+\alpha(E_v-E_F)\},$$

where

$$V = 50 \text{ MeV}, \quad E_F = 8 \text{ MeV}, \quad \alpha = 0.35/V, \quad R = 1.02\, A^{1/3} \text{ fm}. \tag{25}$$

The calculations of the state energies of this potential yields:

$$E_{1s} = 53 \text{ MeV}, \quad E_{1p} = 34 \text{ MeV}, \quad E_{1d} = 17 \text{ MeV}, \tag{26}$$

which are close to the experimental ones.

Within the framework of this model an imaginary part of the hole energy is equivalent to the half-width $\Gamma_v/2$ of the hole state, and may be expressed through the imaginary part of the corresponding optical potential. In our calculation we have used the energy dependence of the imaginary part obtained in Ref. [16] from elastic proton scattering data on nuclei at the energy range of interest

$$W(\varepsilon) = 16.6\{1-\exp(-0.027\varepsilon)\}. \tag{27}$$

Then the widths $\Gamma_v = 2W(E_v)$ turn out to be as follows:

$$\Gamma_{1s} = 20 \text{ MeV}, \quad \Gamma_{1p} = 14 \text{ MeV}, \quad \Gamma_{1d} = 8 \text{ MeV}. \tag{28}$$

In addition, we have here investigated the influence of the nuclear surface diffuseness on the behaviour of the hole state wave function and thus on the $d^4\sigma$ cross sections, having used to this end the Woods-Saxon potential well of the same radius and with the diffuseness parameter $a = 0.65$ fm. The depth of the potential was fitted under the already known set of energies (26).

The knocked-out proton wave function has been calculated in the field of optical potential with parameters, obtained from the corresponding elastic scattering data [17].

$$U(x) = U_c(x) - V \cdot f_1(x) - iWf_2(x),$$

$$f_p(x) = \left[1 + \exp \frac{x - R_p}{a_p}\right]^{-1}, \quad R_p = r_p \cdot A^{1/3}, \tag{29}$$

$$V = 13 \text{ MeV}, \quad W = 11.2 \text{ MeV}, \quad r_1 = 0.92 \text{ fm},$$

$$r_2 = 1\ 45 \text{ fm}, \quad a_1 = 0.42 \text{ fm}, \quad a_2 = 0.46 \text{ fm}.$$

Fig. 1 shows that the optical distortion of the proton wave function influences the nuclear matrix elements rather violently, and this is an essential influence on the absolute cross sections, reducing them three-four times in the given kinematics (Fig. 2).

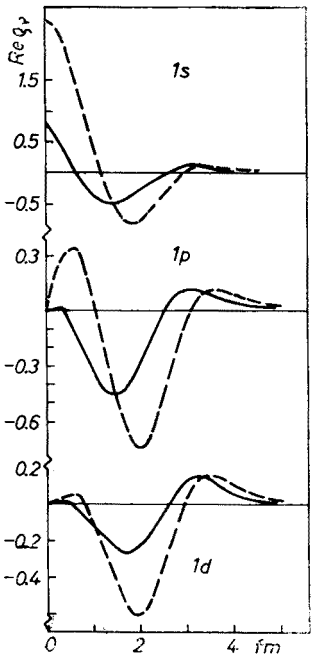

Fig. 1. Behaviour of the real part of the nuclear matrix element. Dotted curves are the plane wave approximation for the knocked-out proton, solid curves — the accounting of the proton optical potential. The hole state functions are in the dynamic square well potential

Furthermore, taking into consideration the electron wave function distortion, we obtain at the same conditions an increase of the quasielastic cross sections, approximately 10% for the 1d peak and 20% for the 1s peak.

Another conclusion has to do with the influence of the form of the hole state potential on calculated cross sections. Moving from the square well wave functions to the realistic Woods-Saxon potential ones, the relative cross sections are changed in the region of 1p

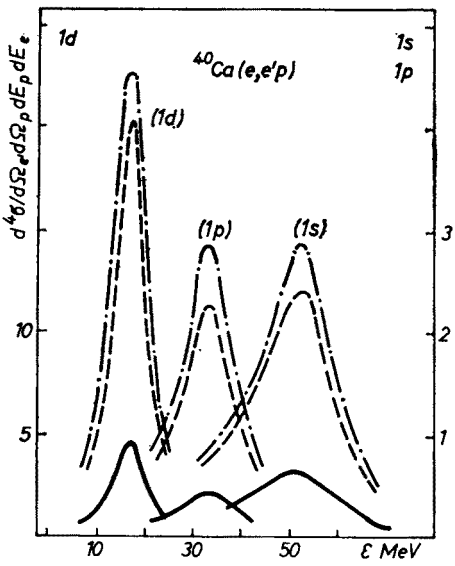

Fig. 2. The cross section of quasi-elastic electron scattering on the 1s, 1p and 1d shells of ^{40}Ca. Dotted curves are the Born approximation, dashed-dotted curves are calculations including the proton and electron distortions. The hole state wave functions are calculated in the dynamic square well potential

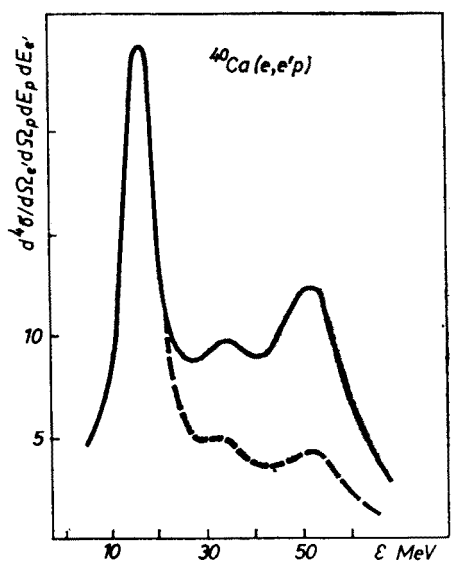

Fig. 3. Influence of the hole state wave function behaviour on the $d^4\sigma$ cross sections. Dotted curve is the calculation for the dynamic square well potential, solid — for the Woods-Saxon potential. In both cases the electron and proton distortions are taken into account. The curves are matched in the pick of the 1d resonance

and 1s peaks approximately two-three times (Fig. 3), which is comparable with the effects of the proton wave distortion. The same results have been obtained in similar calculations of the ^{12}C $(e, e'p)$ reaction [18].

The purpose of the present work was to investigate the usual mechanism of the quasi-elastic $(e, e'p)$ reaction. Now, a comparison of our calculations (Fig. 4) with the existing experimental data leads to the conclusion that despite the nowadays poor experimental

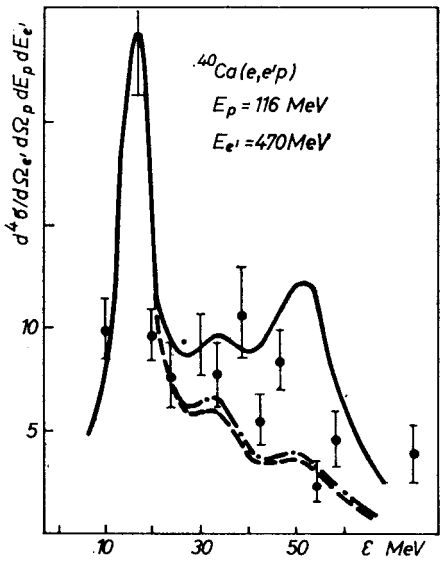

Fig. 4. Comparison of the $d^4\sigma$ cross section with experimental data for ^{40}Ca. Notations are the same as in Fig. 2. The hole state wave functions are calculated in the Woods-Saxon potential. All curves are matched in the pick of the 1d resonance

resolution, the examined mechanism is well justified and can be very useful for the analysis of future experiments that could yield valuable information on the properties of nuclear hole states.

The authors would like to thank V. M. Semenov for consultation and for help in the solution of equations for the bound and continuous state wave functions.

APPENDIX

In the notation of Ref. [11] we express the distortion amplitude and phase functions (8) for the electron part of the reaction amplitude (9) in the framework of the high-energy approximation [9, 10] noting that $k_e \neq k_{e'}$:

$$\Phi(\vec{x}) = \sum_{n=e,e'} \left\{ (1-2\delta_{ne'}) \left[S_n(0) - (\vec{k}_n\vec{x}) \frac{V(0)}{k_n} - \frac{1}{6} a_n(\vec{x}\vec{k}_n) \times \right.\right.$$

$$\left.\left. \times (3k_n'^2 x^2 - 2(\vec{k}_n\vec{x})^2 \right] - d_n[\vec{k}_n\vec{x}]^2 + c_n[\vec{x}\vec{k}_n]^4 \right\}, \qquad \text{(A1)}$$

$$g(\vec{x}) = \frac{k'_e k'_{e'}}{k_e k_{e'}} u^+_{e'} \left\{ 1 + \sum_{n=e,e'} \left(a_n \left[2(\vec{k}_n\vec{x}) - k_n^2 x^2 - \frac{1}{2} k_n (\vec{k}_n x)\vec{\sigma}\vec{x} \right] + \right.\right.$$

$$\left.\left. + (1-2\delta_{ne'}) \left[3d_n(\vec{k}_n\vec{x}) - 10c_n(\vec{k}_n\vec{x}) \left[\vec{k}_n\vec{x}\right]^2 - (d_n k_n + 2c_n k_n [\vec{k}_n\vec{x}]^2)\vec{\sigma}\vec{x} \right] \right) \right\} u_e. \tag{A2}$$

Here $u_{e,e'}$ are the Dirac spinors, so that $\overline{\sum_{(if)}} |u_f^+ u_i|^2 = \cos^2 \vartheta/2$, then $k'_n = k_n(1 - V(0)/E)$, $V(0)$ is determined in [11], and the numerical coefficients a_n, c_n, d_n coincide with a, c, d given in [11], and corresponds to each of the channels e and e'. Then, replacing

$$a_n = \bar{a}/k_n^3, \quad d_n = \bar{d}/k_n^2, \quad c_n = \bar{c}/k_n^4, \tag{A3}$$

where $\bar{a}$, $\bar{c}$, $\bar{d}$ are already independent of energy, we write these functions in the spherical coordinate system $(x, \mu = \cos(\hat{x}, 0z), \varphi)$ with $0z \parallel \vec{q}_1$ (see Eq. (17)):

$$\Phi(x\mu\varphi) = -2V(0)\mu\alpha x - \bar{a}x^3[\mu\alpha - \tfrac{2}{3}\mu^3\alpha^3 - 2\mu\alpha(1-\mu^2)(1-\alpha^2)\cos^2\varphi] -$$

$$- 2\bar{d}x^2[1 - \mu^2\alpha^2 - (1-\mu^2)(1-\alpha^2)\cos^2\varphi] + 2\bar{c}x^4\{(1-\mu^2\alpha^2)^2 +$$

$$+ (1-\mu^2)(1-\alpha^2)[(1-\mu^2)(1-\alpha^2)\cos^2\varphi + 6\mu^2\alpha^2 - 2]\cos^2\varphi\}, \tag{A4}$$

$$g(x\mu\varphi) = \left(1 - \frac{2V(0)k}{k_e k_{e'}}\right) u^+_{e'} \left\{ 1 - \frac{2\bar{a}x^2 k}{k_e k_{e'}} \cdot \left[1 - 2\mu^2\alpha^2 - \right.\right.$$

$$\left.\left. - 2(1-\mu^2)(1-\alpha^2)\cos^2\varphi + 4\frac{\bar{q}}{k}\mu\alpha\sqrt{1-\mu^2}\sqrt{1-\alpha^2}\cos\varphi \right] + \right.$$

$$+ \frac{6\bar{d}xk}{k_e k_{e'}} \left(\alpha\mu - \frac{\bar{q}}{k}\sqrt{1-\mu^2}\sqrt{1-\alpha^2}\cos\varphi \right) + \frac{20\bar{c}x^3 k}{k_e k'_{e'}} \left[-\alpha\mu + \right.$$

$$+ \frac{\bar{q}}{k}\sqrt{1-\mu^2}\sqrt{1-\alpha^2}\cos\varphi + \mu^3\alpha^3 - \frac{3\bar{q}}{k}\mu^2\alpha^2\sqrt{1-\mu^2}\sqrt{1-\alpha^2}\cos\varphi +$$

$$\left. + 3\alpha\mu(1-\mu^2)(1-\alpha^2)\cos^2\varphi - \frac{\bar{q}}{k}(1-\alpha^2)^{3/2}(1-\mu^2)^{3/2}\cos^3\varphi \right] +$$

$$+ \left[\frac{\bar{a}xk}{2k_e k_{e'}} \left(2\mu\alpha\frac{\bar{q}}{k} - 2\sqrt{1-\mu^2}\sqrt{1-\alpha^2}\cos\varphi \right) + \frac{4\bar{c}x^2 k}{k_e k_{e'}} \times \right.$$

$$\times \left(-\frac{\bar{q}}{k} + \frac{\bar{q}}{k}\mu^2\alpha^2 - 2\mu\alpha\sqrt{1-\mu^2}\sqrt{1-\alpha^2}\cos\varphi + \right.$$

$$\left.\left. + \frac{\bar{q}}{k}(1-\mu^2)(1-\alpha^2)\cos^2\varphi \right) - \frac{2\bar{d}\bar{q}}{k_e k_{e'}} \right] \vec{\sigma}\vec{x} \left. \right\} u_e. \tag{A5}$$

Particularly in the case of elastic scattering, when $k_e = k_{e'}$, the functions (A1)–(A5) coincide with those given in Ref. [11].

REFERENCES

[1] W. Czyż, K. Gottfried, *Ann. Phys. (N. Y.)* **21**, 47 (1963); T. de Forest, Jr., *Ann. Phys.* **45**, 365 (1967).
[2] U. Amaldi et al., *Phys. Lett.* **22**, 593 (1966).
[3] V. K. Tartakovsky, A. A. Pasichny, Preprint ITF–70–38, Kiev 1970.
[4] V. V. Balashov, D. V. Meboniya, *Izv. Akad. Nauk Arm. SSR, Ser. Fiz.* **3**, 122 (1968).
[5] V. V. Balashov, N. M. Kabachnik, V. I. Markov, *Nucl. Phys.* **A129**, 369 (1969).
[6] G. M. Vagradov, V. V. Gorchakov, *Kratkiye Soobshcheniya po Fizike FIAN*, **6**, 26 (1970); **8**, 66 (1970).
[7] G. M. Vagradov, B. N. Kalinkin, *Teor. Mat. Fiz.* **9**, 240 (1971).
[8] G. M. Vagradov, V. V. Gorchakov, *Izv. Akad. Nauk SSSR, Ser. Fiz.* **36**, 680 (1972).
[9] D. R. Yennie, F. L. Boos, D. S. Ravenhall, *Phys. Rev.* **137B**, 822 (1965).
[10] Yu. S. Pol', V. K. Lukyanov, I. Z. Petkov, *Acta Phys. Pol.* **34**, 50 (1968).
[11] I. Z. Petkov, V. K. Lukyanov, Yu. S. Pol', *Yad. Fiz.* **6**, 57 (1966).
[12] I. Z. Petkov, V. K. Lukyanov, Yu. S. Pol', *Yad. Fiz.* **4**, 556 (1966).
[13] A. N. James et al., *Nucl. Phys.* **A138**, 145 (1969).
[14] G. Landaud et al., *Nucl. Phys.* **A173**, 337 (1971).
[15] S. Hiramatsu et al., *International conference*, SENDAI, Japan, September 12–15 (1972).
[16] K. Seth, *Nucl. Phys.* **A138**, 61 (1969).
[17] A. Ingemarsson, G. Tibell, *Phys. Scripta* **4**, 235 (1971).
[18] S. Radhakant, *Phys. Lett.* **40B**, 70 (1972).